0022-3565/04/3083-805–813$20.00
THE JOURNAL OF PHARMACOLOGY AND EXPERIMENTAL THERAPEUTICS
JPET 308:805–813, 2004

Vol. 308, No. 3
58792/1128131
Printed in U.S.A.

Mammalian Voltage-Gated Calcium Channels Are Potently Blocked by the Pyrethroid Insecticide Allethrin

Michael E. Hildebrand, John E. McRory,[1] Terrance P. Snutch, and Anthony Stea

Biotechnology Laboratory, University of British Columbia, Vancouver, British Columbia, Canada (M.E.H., J.E.M., T.P.S.); and University-College of the Fraser Valley, Abbotsford, British Columbia, Canada (A.S.)

Received August 18, 2003; accepted November 14, 2003

ABSTRACT

Pyrethroids are commonly used insecticides for both household and agricultural applications. It is generally reported that voltage-gated sodium channels are the primary target for toxicity of these chemicals to humans. The phylogenetic and structural relatedness between sodium channels and voltage-gated calcium (Ca) channels prompted us to examine the effects of the type 1 pyrethroid allethrin on the three major classes of mammalian calcium channels exogenously expressed in human embryonic kidney 293 cells. We report that all classes of mammalian calcium channels are targets for allethrin at concentrations very similar to those reported for interaction with sodium channels. Allethrin caused blockade with IC_{50} values of 7.0 μM for T-type α_{1G} ($Ca_v3.1$), 6.8 μM for L-type α_{1C} ($Ca_v1.2$), and 6.7 μM for P/Q-type α_{1A} ($Ca_v2.1$) channels. Mechanistically, the blockade of calcium channels was found to be significantly different than the prolonged opening of mammalian sodium channels caused by pyrethroids. In all calcium channel subtypes tested, allethrin caused a significant acceleration of the inactivation kinetics and a hyperpolarizing shift in the voltage dependence of inactivation. The high-voltage-activated P/Q- and L-type channels showed a frequency of stimulation-dependent increase in block by allethrin, whereas the low-voltage-activated α_{1G} subtype did not. Allethrin did not significantly modify the deactivation kinetics or current-voltage relationships of any of the calcium channel types. Our study indicates that calcium channels are another primary target for allethrin and suggests that blockade of different types of calcium channels may underlie some of the chronic effects of low-level pyrethroid poisoning.

The use of pyrethroid insecticides (synthetic forms of natural toxins called pyrethrins that are produced by *Chrysanthemum* sp.) is commonplace. Pyrethroids are found in household insecticidal sprays and in preparations for agricultural use (Zlotkin, 1999; Kumari et al., 2002; Soderlund et al., 2002). Recently, to minimize the transmission of the West Nile virus, pyrethroids have been used or considered for use to destroy both larval and adult mosquitoes in many areas throughout North America (Thier, 2001). Due to this widespread use, pyrethroid contamination has become a potential problem. Even in urban centers, the presence of pyrethroid metabolites has been identified in humans (Schettgen et al., 2002). Although a primary reason for the ubiquitous use of pyrethroids is their relatively low acute mammalian toxicity (Zlotkin, 1999), these agents are considered poisonous and can affect the nervous system, causing symptoms that range from whole-body tremors to convulsions that sometimes result in death. Usually, pyrethroids are used at levels that prevent acute poisoning, but these lower levels may stimulate chronic effects when exposure is prolonged or recurrent (Abou-Donia et al., 2001). Since the primary target for the insecticidal action of pyrethroids are insect voltage-gated sodium channels, it is generally believed that mammalian sodium channels are also the primary targets for toxicity in humans (Motomura and Narahashi, 2001; Soderlund and Lee, 2001; Spencer et al., 2001;Wang et al., 2001; de la Cerda et al., 2002). Other potential molecular targets for pyrethroids include chloride channels, ATPases, GABA receptors, glutamate receptors, acetylcholine receptors, and voltage-gated calcium channels (Hagiwara et al., 1988; Satoh, 1995; Forshaw et al., 2000; Soderlund et al., 2002; Kakko et al., 2003). Calcium channels play essential roles in nerve cell excitability, calcium homeostasis, synaptic signaling, and gene expression modulation (Sutton et al., 1999; Catterall, 2000; Dolmetsch et al., 2001; McRory et al., 2001; Perez-Reyes, 2003). Voltage-gated calcium

This work was supported by a grant from the Canadian Institute for Health Research (CIHR) and a CIHR Senior Scientist Award (to T.P.S.), fellowship support from the Natural Sciences and Engineering Research Council of Canada and the Michael Smith Foundation for Health Research (to M.E.H.), and research funding from the University-College of the Fraser Valley (to A.S.).

[1] Present address: Department of Physiology and Biophysics, Cellular and Molecular Neurobiology Research Group, University of Calgary, Calgary, Alberta, Canada.

Article, publication date, and citation information can be found at http://jpet.aspetjournals.org.
DOI: 10.1124/jpet.103.058792.

ABBREVIATION: HEK, human embryonic kidney.

channels can be divided into three major groups based on their physiological, pharmacological, and molecular properties (for review, see Catterall, 2000).

In the present study, we have undertaken a comprehensive analysis of the effects of the type I pyrethroid allethrin on three different classes of calcium channels: *i*) a high-voltage activated L-type calcium channel (α_{1C}/$Ca_v1.2$) that is known to be involved with excitation-contraction coupling in the heart, hormone secretion, calcium signaling, and gene regulation (Catterall, 2000; Dolmetsch et al., 2001); *ii*) a high-voltage activated P/Q-type channel (α_{1A}/$Ca_v2.1$) that is essential for synaptic signaling (Sutton et al., 1999; Catterall, 2000); and *iii*) a low-voltage activated T-type calcium channel (α_{1G}/$Ca_v3.1$) that is essential for modulating electrical signals in the nervous system (Catterall, 2000; McRory et al., 2001; Perez-Reyes, 2003). Because of the phylogenetic and structural relatedness between sodium and calcium channels, we hypothesized that allethrin might have significant effects on the properties of calcium channels in the same range of concentrations that sodium channel properties are affected. A detailed examination of the effects of allethrin on these three types of calcium channels may help to explain some of the symptoms and potential dangers of low-level chronic exposure to pyrethroids and provide more information about the risk factors associated with the use of these insecticidal chemicals.

Materials and Methods

Cell Culture. Human embryonic kidney (HEK 293; tsA201) cells were grown in standard Dulbecco's modified Eagle's medium + 10% fetal bovine serum and 50 U/ml penicillin-streptomycin to 80% confluence and maintained at 37°C in a humidified incubator with 95% atmosphere and 5% CO_2. A stable cell line expressing α_{1G} was generated by transfecting linearized rat α_{1G} (in pCDNA3.1 vector) into HEK cells using standard calcium-phosphate precipitation, and recombinant clones were selected with zeocin. Other HEK cells were transiently transfected with either rat α_{1A} or rat α_{1C} (6 μg in pcDNA3.1 vector) and β_{1b}, $\alpha_2\delta$, and CD8 marker plasmids at a 1:1:1:0.25 M ratio using LipofectAMINE (Invitrogen, Carlsbad, CA). Twenty-four hours after transfections, cells were transferred to a 28°C incubator. In some experiments, human α_{1A} was transfected instead of rat α_{1A}. Transiently transfected cells were selected for expression of CD8 by adherence of Dynabeads (Dynal Biotech, Lake Success, NY). The stable α_{1G} cell line was enzymatically dissociated with trypsin-EDTA and plated on 35-mm culture dishes 12 to 24 h before recordings, whereas recordings on α_{1A} and α_{1C} cells occurred 36 to 72 h after transient transfections.

Electrophysiological Recordings. Macroscopic currents were recorded using the whole-cell patch-clamp technique (Hamill et al., 1981). The external recording solution contained 2 mM $BaCl_2$, 1 mM $MgCl_2$, 10 mM HEPES, 40 mM tetraethylammonium-Cl, 92 mM CsCl, and 10 mM glucose, pH 7.2. The internal pipette solution contained 120 mM $CsCl_2$, 1 mM $CaCl_2$, 11 mM EGTA , 10 mM HEPES , 2 mM Mg-ATP, pH 7.2. Whole-cell currents were recorded using an Axopatch 200A amplifier (Axon Instruments Inc., Union City, CA) and controlled and monitored with a personal computer running pCLAMP software version 6.03 (Axon Instruments Inc.). Patch pipettes (borosilicate glass BF150–86-10; Sutter Instrument Company, Novato, CA) were pulled using a microforge (Narishige, Tokyo, Japan) with typical resistances of 3 to 7 MΩ when filled with internal solution. The bath was connected to the ground via a 3 M KCl agar bridge. Whole-cell currents that exceeded 2 nA were not examined, minimizing voltage error (<2–3 mV). Only cells exhibiting adequate voltage control [judged by a smoothly rising current-voltage (*I-V*) relationship and monoexponential decay of capacitive currents] were included in the analysis. All recordings were performed at room temperature (20–24°C). Data were low-pass filtered at 2 kHz using the built-in Bessel filter of the amplifier, and the amplifier was also used for whole-cell capacitance compensation on every cell. In some cases, subtraction of capacitance and leakage current was performed online using a P/4 protocol.

Recording Protocols. The time course of allethrin effects were investigated using 80 to 400 ms steps to peak potentials every 5 s from a holding potential of −100 mV. Typically, peak test potentials were −30 mV for α_{1G}, −10 mV for α_{1A}, and −5 mV for α_{1C}. For the allethrin concentration-response experiments, holding potentials of −100, −80, and −60 mV were used for the α_{1G}, α_{1A}, and α_{1C} channels, respectively. To examine the frequency dependence of allethrin block (at a holding potential of −100 mV), no depolarizations were performed for the first 3 min (0.0056 Hz) of allethrin perfusion, followed by depolarizations to peak potentials every 15 s (0.067 Hz). Allethrin block was also measured with depolarizations to peak potentials every 5 s (0.20 Hz) or every 2 s (0.5 Hz) from a holding potential of −100 mV. For the higher stimulation frequency protocols, any current rundown was allowed to equilibrate before allethrin was applied. Current-voltage relations were measured by a series of depolarizing pulses applied from a holding potential of −100 mV to membrane potentials increasing at 5 mV increments. Deactivation was examined through analysis of tail currents following brief steps (6–20 ms) to peak potentials. Inactivation curves were obtained by applying depolarizations to peak test potentials at the end of 10-s prepulses ranging from −120 to +20 mV at 10 mV increments (total time between sweeps = 15 s). Unless otherwise stated in the text, the holding potential for all the experiments was −100 mV.

Data Analysis. Recordings were analyzed using Clampfit 6.03 (Axon Instruments). This included leak subtraction on cells that were not subtracted online and low-pass filtering at 1000 kHz. Figures and fittings used the software program Microcal Origin (version 6.0; OriginLab Corp., Northampton, MA). Data from allethrin concentration-response studies were fitted with the equation $y = [(A_1 - A_2)/\{1 + (x/x_o)^P\} + A_2]$, where A_1 is initial (= 0), A_2 is final block value, x_o is IC_{50} (concentration causing 50% inhibition of currents), and P (Hill coefficient) gives a measure of the steepness of the curve. Time courses of channel blockade, activation, and inactivation rates during steps to peak potential and deactivation of currents following brief test pulses were well described by single exponential curves to give time constant values cited in the text (τ_{on}, τ_{off}, τ_{act}, τ_{inact}, and τ_{deact}). Steady-state inactivation curves were constructed by plotting the normalized current during the test pulse as a function of the prepulse potential. The data were fitted with the Boltzmann equation $I/I_{max} = [1 + \exp(\{V - V_{50inact}\}/k_i)]^{-1}$, where I is the peak current when the prepulse potential is most hyperpolarized, V is the prepulse potential, $V_{50inact}$ is the half-inactivation potential, and k_i is the inactivation slope factor. Current-voltage relationships were fitted with the modified Boltzmann equation $I = [G_{max} \cdot (V_m - E_{rev})]/[1 + \exp(\{V_m - V_{50act}\}/k_a)]$, where V_m is the test potential, V_{50act} is the half-activation potential, E_{rev} is the extrapolated reversal potential, G_{max} is the maximum slope conductance, and k_a reflects the slope of the activation curve. Statistical significance was determined by Student's t tests, and significant values were set at $p < 0.01$ or as indicated in the text and figure legends.

Solutions and Drugs. A mixture of allethrin stereoisomers was obtained from Sigma-Aldrich (St. Louis, MO), and a 50 mM concentrated stock solution was prepared in dimethyl sulfoxide. Test solutions containing allethrin were prepared fresh for each experiment by adding calculated amounts of the concentrated stock solution to the external recording solution. The syringes that contained the allethrin recording solutions were wrapped in foil throughout the experiments to prevent degradation of the allethrin caused by light exposure. The highest concentration of dimethyl sulfoxide in the recording solution did not exceed 0.1%, a concentration that did not detectably affect calcium channel properties. The perfusion system

consisted of a custom-made multiple solution perfusion manifold with four input and output capillary tubes (custom microfil, 28 gauge, 250 μm inner diameter and 350 μm outer diameter; World Precision Instruments, New Haven, CT) ensheathed in a glass pipette. High chemical-resistant Tygon Chemfluor FEP (Norton Performance Plastics, Akron, OH) and Silastic tubing (Fisher Scientific Co., Pittsburgh, PA) were used to connect the perfusion manifold to the syringe valve. Gravity-driven perfusion occurred at a rate of approximately 400 μl/min, and the outputs of the manifold were placed within close proximity of the cell, resulting in the cell being bathed in new solutions with minimal delay (within 1 s).

Results

Type I Pyrethroid Allethrin Potently Blocks Voltage-Gated Calcium Channels. The expression of cloned voltage-gated calcium channels in HEK cells has allowed the comprehensive analysis of the different subtypes in both electrophysiological and pharmacological studies (for review, see Catterall, 2000). The prolonged opening of mammalian sodium channels induced by pyrethroids has been well documented (Motomura and Narahashi, 2001; Soderlund and Lee, 2001; Spencer et al., 2001; Wang et al., 2001; de la Cerda et al., 2002), but the blockade of calcium channels has not been well characterized (Hagiwara et al., 1988; Satoh, 1995). Using the HEK expression system, we analyzed the effects of different concentrations of the type I pyrethroid allethrin on three distinct calcium channel subtypes: *i*) a low-voltage activated T-type channel, α_{1G} ($Ca_v3.1$); *ii*) a high-voltage activated P/Q-type channel, α_{1A} ($Ca_v2.1$); and *iii*) a dihydropyridine-sensitive, high-voltage activated L-type channel, α_{1C} ($Ca_v1.2$). Unlike the pyrethroid-induced prolonged opening of sodium channels, all three calcium channel subtypes were significantly blocked by 10 to 20 μM allethrin (Fig. 1).

To better quantify the blocking efficiency of allethrin, a concentration-response curve was generated by exposing the whole cell barium currents to varying concentrations of allethrin (Fig. 1D). The peak currents were blocked in a dose-dependent manner, generating IC_{50} values of 7.0 μM (α_{1G}), 6.8 μM (α_{1C}), and 6.7 μM (α_{1A}). The Hill coefficient (*P*) determined from the concentration-response curves was 2.5 for α_{1G}, 1.3 for α_{1C}, and 1.3 for α_{1A}. These IC_{50} values for allethrin on calcium channels are in the same range as has previously been reported for several types of pyrethroids (including allethrin) acting on mammalian sodium channels (Ginsburg and Narahashi, 1999; Motomura and Narahashi, 2001; Soderlund and Lee, 2001; Spencer et al., 2001;Wang et al., 2001; de la Cerda et al., 2002).

Application of allethrin with a fast perfusion system showed that this pesticide rapidly blocks α_{1G} (τ_{on} = 17.8 ±

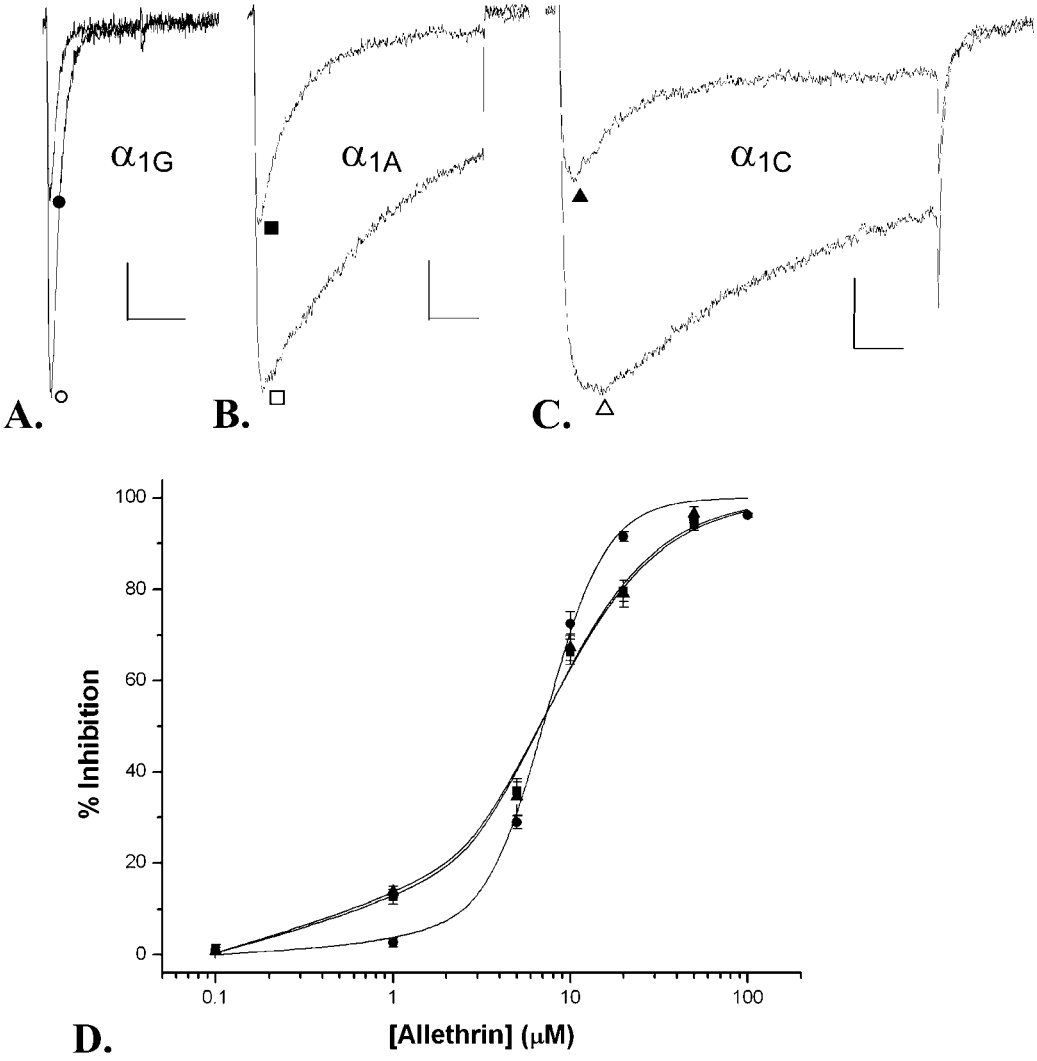

Fig. 1. Voltage-gated calcium channels are potently blocked by the type I pyrethroid allethrin. A, a representative current trace (voltage step −100 to −30 mV) shows that application of 10 μM allethrin (filled circles) blocks on average 72.5% (±2.7%; n = 16) of the α_{1G} whole-cell calcium current (open circles represents untreated control current). B, application of 20 μM allethrin (filled squares) blocks on average 50.4% (±3.0%; n = 16) of the α_{1A} current (voltage step −100 to −10 mV). C, application of 20 μM allethrin (filled triangles) blocks on average 67.4% (±3.8%; n = 10) of the α_{1C} current (voltage step −100 to −5 mV). Note the scale for the current traces; y-axis = 50 (A) or 100 p*A* (B and C), x-axis = 50 ms. D, a concentration-response curve shows that allethrin blocks calcium channels with the following IC_{50} values calculated from the smooth curve: *i*) α_{1G} = 7.0 μM (filled circles; slope factor (P) = 2.5; holding potential −100 mV); *ii*) α_{1C} = 6.8 μM (filled triangles; slope factor = 1.3; holding potential −60 mV); and *iii*) α_{1A} = 6.7 μM (filled squares; slope factor = 1.3; holding potential −80 mV). Note that 4 to 16 cells were sampled for each data point with the mean and S.E. shown on the graph.

1.9 s, $n = 4$), α_{1A} ($\tau_{on} = 15.9 \pm 2.7$ s, $n = 5$), and α_{1C} currents ($\tau_{on} = 26.2 \pm 1.9$ s, $n = 6$). The allethrin blockade is readily and rapidly reversible for all three types of calcium channels (Fig. 2; α_{1G} $\tau_{off} = 17.8 \pm 2.9$ s, $n = 4$; α_{1A} $\tau_{off} = 17.3 \pm 3.8$ s, $n = 5$; α_{1C} $\tau_{off} = 49.8 \pm 3.9$ s, $n = 6$).

Allethrin Blockade of High Voltage-Activated Calcium Channels Is Frequency- and Voltage-Dependent. Pyrethroids show a frequency of stimulation-dependent increase in their effects on voltage-gated sodium channel activity (Vais et al., 2001, 2003; Wang and Wang, 2003). By changing the frequency of test pulses from once after 3 min to once every 2 s, we saw significant increases in the potency of block of α_{1A} and α_{1C} currents by allethrin but no significant change in the block of α_{1G} currents (Fig. 3). In addition to altering the frequency of stimulation, we also changed the holding potentials and tested whether allethrin block altered the potency. Changing the holding potential from −100 to −80 mV caused no significant change in the blockade by 10 μM allethrin for α_{1G} currents (−100 mV = 76.3 ± 3.2% block, $n = 10$; −80 mV = 78.0 ± 2.8% block, $n = 9$). However, changing the holding potential from −100 to −80 mV caused a significant change ($p < 0.01$) in the blockade by 20 μM allethrin for α_{1A} currents (−100 mV = 60.9 ± 2.9% block, $n = 15$; −80 mV = 77.9 ± 3.5% block, $n = 8$). Changing the holding potential from −100 to −60 mV also caused a significant change ($p < 0.01$) in the blockade by 10 μM allethrin for α_{1C} currents (−100 mV = 35.4 ± 2.1% block, $n = 9$; −60 mV = 68.3 ± 3.0% block, $n = 8$). Since allethrin blockade was dependent on holding potential, the concentration-response curve was generated at the holding potential (−100 mV for α_{1G}, −80 mV for α_{1A}, and −60 mV for α_{1C}) where minimal inactivation of each current was expected (Fig. 1D).

Allethrin Alters Kinetics of Calcium Channels. Pyrethroids show a pronounced effect on the kinetics of both insect and mammalian sodium channels (for review, see Zlotkin, 1999; Vais et al., 2001; Soderlund et al., 2002). In these studies, a pronounced slowing of the inactivation rate was observed upon exposure to pyrethroids. In our study, after partial blockade by allethrin, the α_{1A} and α_{1C} currents had a visibly faster rate of inactivation compared with control currents (Fig. 1, B and C). The rates of inactivation were analyzed by fitting the currents with single exponential curves and determining the time constant of inactivation (τ_{inact}). T-type α_{1G} currents are normally fast inactivating ($\tau_{inact} = 9.2 \pm 0.2$ ms, $n = 39$; Fig. 1A) compared with the P/Q-type α_{1A} currents ($\tau_{inact} = 126.4 \pm 6.5$ ms, $n = 33$; Fig. 1B) and

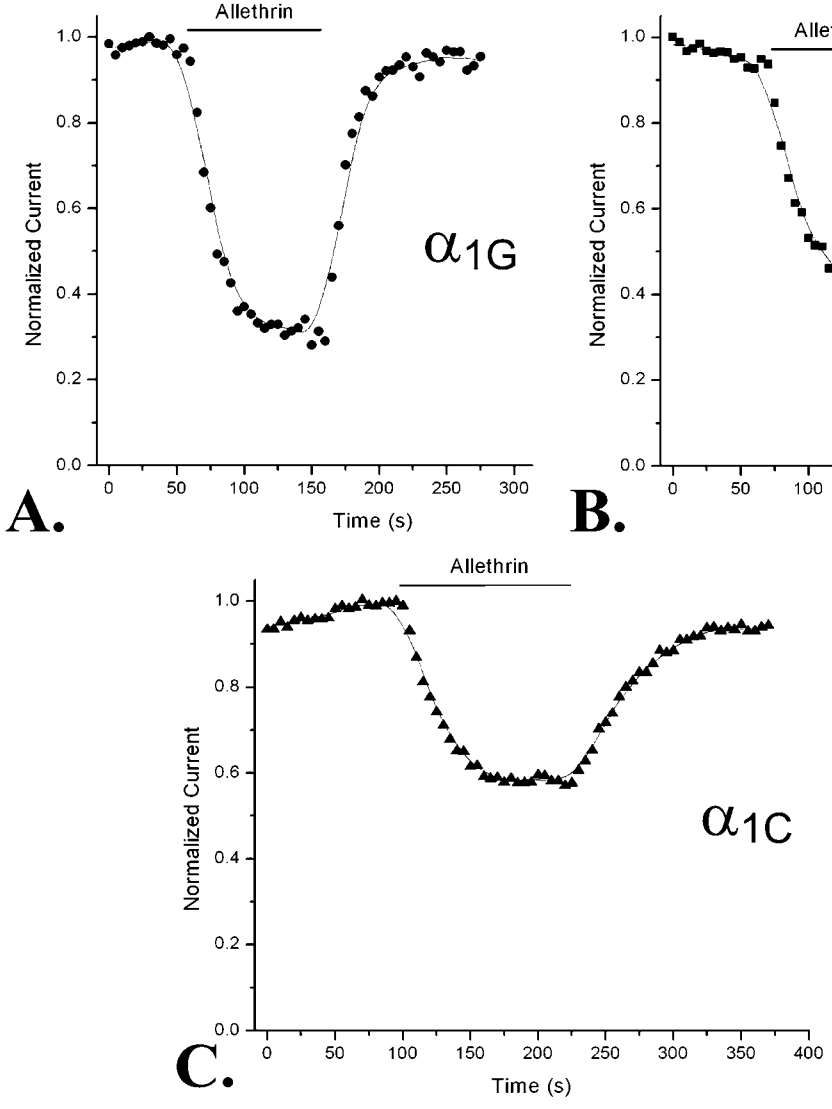

Fig. 2. Allethrin blockade of calcium channels is completely reversible. A, application of 10 μM allethrin reversibly blocks the α_{1G} current; B, 20 μM allethrin reversibly blocks α_{1A} currents; C, 10 μM allethrin reversibly blocks α_{1C} currents. Note that allethrin was added corresponding to the length of time indicated by the solid bar above the graphs. The whole-cell current values for each point were divided by the maximal current to give normalized current on the y-axis of each graph.

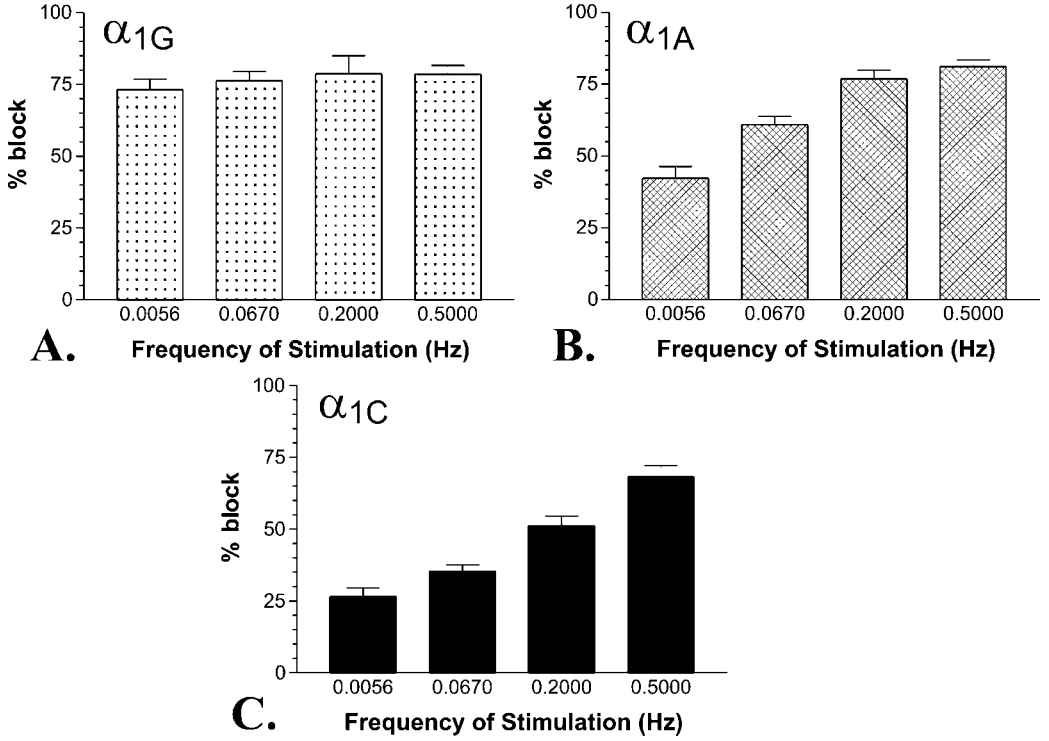

Fig. 3. High-voltage activated calcium channels show frequency-dependent blockade by allethrin. A, the blockade of low-voltage activated α_{1G} currents by 10 μM allethrin is unaffected by the frequency of the test pulses. A test pulse after 3 min (0.0056 Hz) causes about the same block as test pulses every 2 s (0.5 Hz). B, the blockade of high-voltage activated α_{1A} currents by 20 μM allethrin is significantly affected by the frequency of the test pulses. A test pulse after 3 min (0.0056 Hz) showed a 42% block by allethrin, whereas higher frequency stimulation (0.5 Hz) caused a significantly greater block (81%; $p < 0.01$). C, the blockade of high-voltage activated α_{1C} currents by 10 μM allethrin is significantly affected by the frequency of the test pulses. A test pulse after 3 min (0.0056 Hz) showed a 27% block by allethrin, whereas higher frequency stimulation (0.5 Hz) caused a significantly greater block (68%; $p < 0.01$). Note that 6 to 15 cells were sampled for each bar in the graphs above.

slowly inactivating L-type α_{1C} currents (τ_{inact} = 274.6 ± 27.6 ms, n = 23; Fig. 1C). After 10 μM allethrin treatment, the α_{1G} currents inactivated 31% faster than untreated α_{1G} controls, and the effect on inactivation was concentration-dependent (Fig. 4A). Allethrin (10 μM) caused a more dramatic increase in the inactivation rate of the P/Q-type currents (54%; Fig. 4B) and L-type currents (67%; Fig. 4C), but, as with the T-type currents, the acceleration of the inactivation rate was dependent on the applied allethrin concentration (Fig. 4).

The application of allethrin also caused a small increase in the activation rate (τ_{act}) of the calcium channels (Fig. 1), but this increase was not significantly different for the α_{1G} currents (control τ_{act} = 1.34 ± 0.07 ms, n = 14; 10 μM allethrin τ_{act} = 1.23 ± 0.10, n = 14). The activation acceleration was significant for the α_{1A} currents (control τ_{act} = 1.96 ± 0.19 ms, n = 15; 20 μM allethrin τ_{act} = 1.34 ± 0.11, n = 15; $p < 0.01$) and α_{1C} currents (control τ_{act} = 3.41 ± 0.22 ms, n = 15; 10 μM allethrin τ_{act} = 2.24 ± 0.18, n = 15; $p < 0.01$) exposed to allethrin.

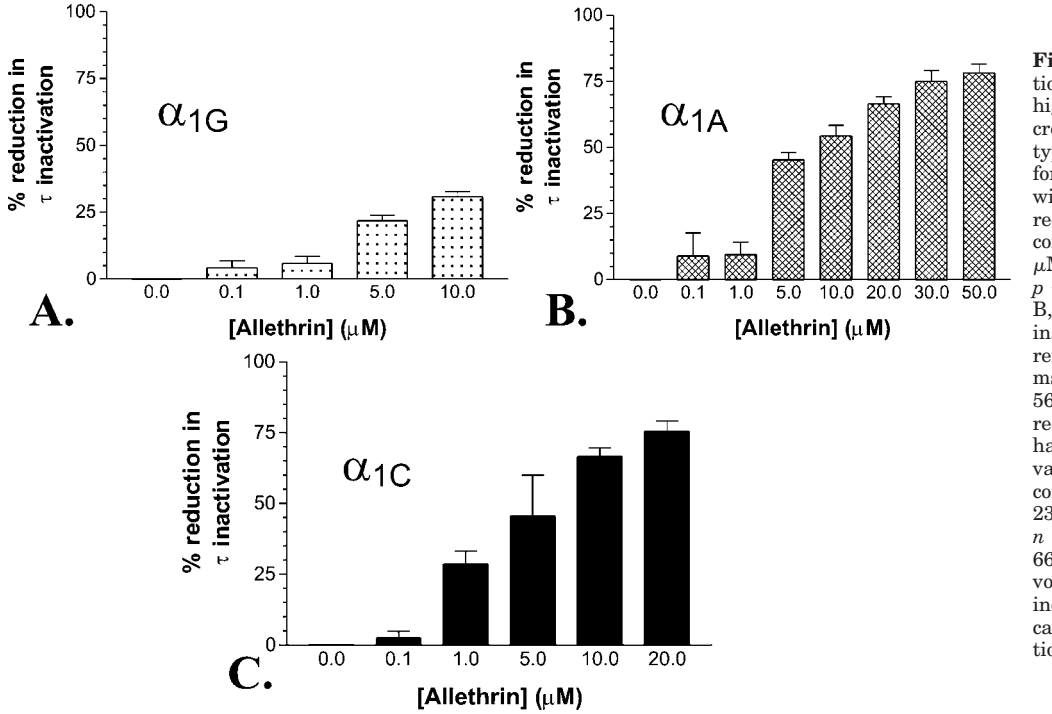

Fig. 4. Allethrin increases inactivation rates of calcium channels. A, higher concentrations of allethrin increases the speed of inactivation of T-type α_{1G} currents. The time constants for inactivation (τ_{inact}) were compared with control values and the percent reduction plotted on the graph (e.g., control τ_{inact} = 9.2 ± 0.2 ms, n = 39; 10 μM allethrin τ_{inact} = 6.0 ± 0.2, n = 16; $p < 0.01$; percent reduction = 30.8%). B, allethrin has a greater effect on inactivation of the P/Q-type α_{1A} currents (e.g., control τ_{inact} = 126.4 ± 6.5 ms, n = 33; 10 μM allethrin τ_{inact} = 56.6 ± 1.6, n = 7; $p < 0.01$; percent reduction = 54.3%). C, allethrin also has a pronounced effect on the inactivation of the L-type α_{1C} currents (e.g., control τ_{inact} = 274.6 ± 27.6 ms, n = 23; 10 μM allethrin τ_{inact} = 92.1 ± 9.9, n = 14; $p < 0.01$; percent reduction = 66.7%). Note that in all three types of voltage-gated calcium channels, the increase in the inactivation rate caused by allethrin was concentration-dependent.

The most obvious effect of pyrethroid insecticides on sodium channels is a distinct slowing of deactivation of the tail currents (for review see Zlotkin, 1999; Vais et al., 2001; Soderlund et al., 2002). We tested the deactivation properties of the calcium channels upon exposure to allethrin. Unlike that found for sodium channels, it is clear from Fig. 1 that exposure to 10 to 20 μM allethrin did not significantly alter the deactivation properties of any of the three types of calcium channels (α_{1G} − control τ_{deact} = 1.11 ± 0.05 ms, n = 7; 10 μM allethrin τ_{deact} = 1.11 ± 0.03 ms, n = 7; α_{1A} − control τ_{deact} = 0.47 ± 0.07 ms, n = 11; 20 μM allethrin τ_{deact} = 0.48 ± 0.07 ms, n = 11; α_{1C} − control τ_{deact} = 0.97 ± 0.12 ms, n = 12; 10 μM allethrin τ_{deact} = 1.09 ± 0.16 ms, n = 12).

Allethrin Affects Voltage-Dependent Inactivation but Not Activation of Voltage-Gated Calcium Channels. Since pyrethroid insecticides have been shown to affect the voltage-dependent properties of sodium channels (Smith et al., 1998; Spencer et al., 2001; de la Cerda et al., 2002), we tested the effects of allethrin on the voltage-dependent properties of the three calcium channel subtypes. In general, T-type calcium channels (e.g., α_{1G}) inactivate at more hyperpolarized potentials than P/Q-type (α_{1A}) or L-type (α_{1C}) channels. The untreated α_{1G} currents were half-inactivated at a holding potential of −74 mV, whereas the α_{1A} and α_{1C} currents were half-inactivated at a potential of −54 mV and −34 mV, respectively (Fig. 5). We examined the effects of allethrin on the voltage-dependent inactivation of the calcium channels. Application of allethrin caused a large hyperpolarized shift in the voltage-dependent inactivation of the α_{1G} (~13 mV), α_{1A} (~32 mV), and α_{1C} (~19 mV) currents (Fig. 5).

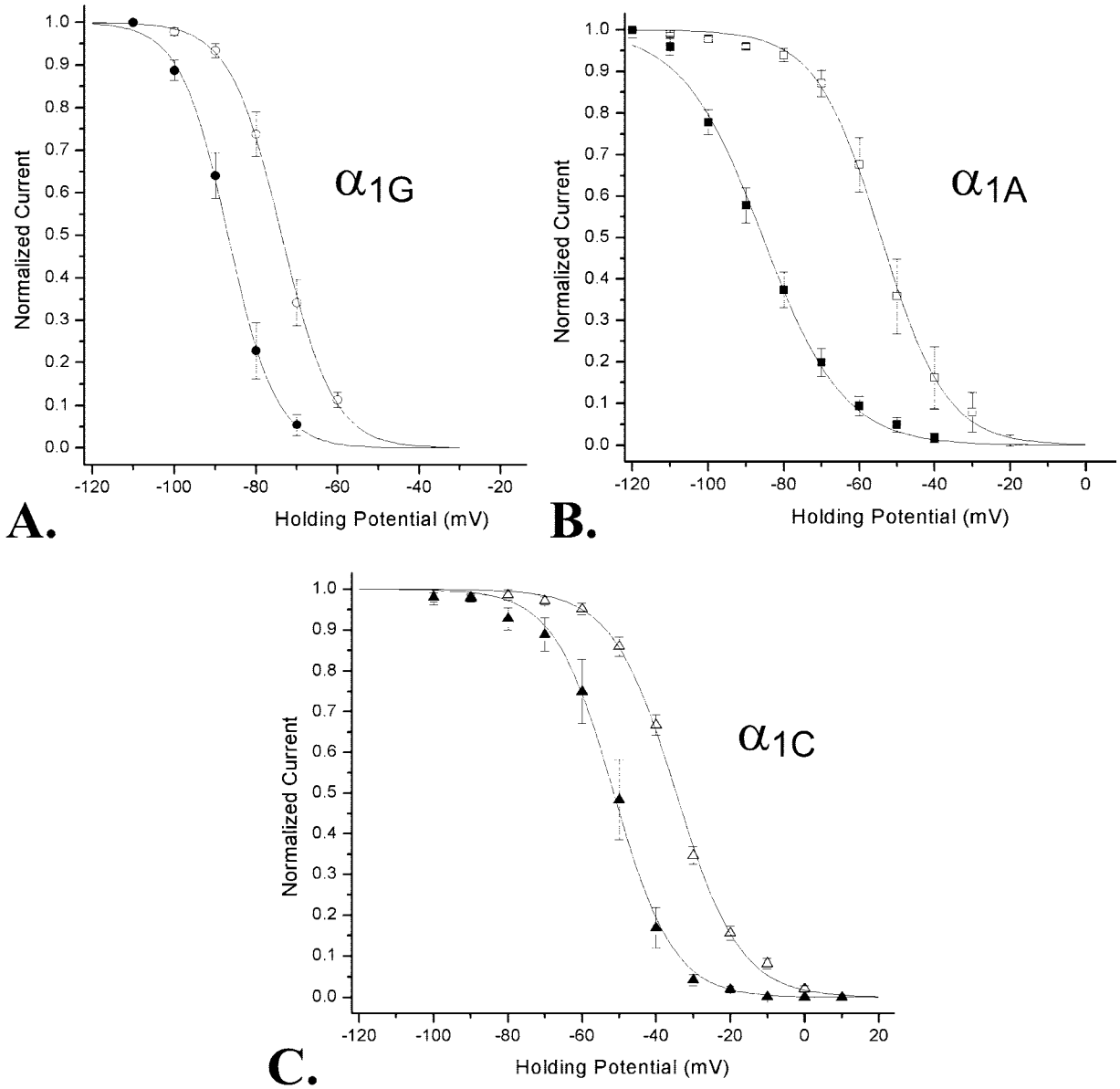

Fig. 5. Allethrin shifts the voltage-dependent inactivation of calcium channels. A, the voltage-dependent inactivation of the α_{1G} currents caused a hyperpolarized shift of approximately 13 mV when exposed to allethrin (control $V_{50inact}$ = −73.9 ± 1.4 mV, n = 7; 10 μM allethrin $V_{50inact}$ = −86.5 ± 1.6 mV, n = 7; $p < 0.01$). B, allethrin causes an even larger (~32 mV) hyperpolarized shift of inactivation for α_{1A} currents (control $V_{50inact}$ = −53.8 ± 2.7 mV, n = 8; 20 μM allethrin $V_{50inact}$ = −86.1 ± 2.7 mV, n = 8; $p < 0.01$). C, allethrin also causes a significant hyperpolarized shift of inactivation (~19 mV) for α_{1C} currents (control $V_{50inact}$ = −33.7 ± 0.8 mV, n = 9; 10 μM allethrin $V_{50inact}$ = −52.5 ± 2.1 mV, n = 9; $p < 0.01$). Note that in all three graphs shown above, allethrin-treated cells are shown with filled symbols whereas controls are shown with open symbols. The whole-cell current values for each point were divided by the maximal current to give normalized current on the y-axis of each graph.

A key distinguishing characteristic of T-type channels is the low voltages required for activation of the channels compared with high-voltage activated channels like the P/Q- and L-type channels. Under control conditions, the α_{1G} currents activated at relatively hyperpolarized potentials (V_{50act} = −41.3 ± 0.7 mV, n = 12) compared with the α_{1A} (V_{50act} = −19.3 ± 1.6 mV, n = 9; Fig. 6) and α_{1C} currents (V_{50act} = −13.9 ± 1.5 mV, n = 13; Fig. 6). As shown in Fig. 6, allethrin did not cause any significant shift in the voltage-dependent activation of the three types of calcium channels studied.

Discussion

Voltage-Gated Calcium Channels Are Another Primary Target for Pyrethroid Toxicity. It has been generally assumed that the symptoms of acute toxicity of pyrethroid pesticides in humans is caused by their action on voltage-gated sodium channels (for review, see Zlotkin, 1999; Vais et al., 2001; Soderlund et al., 2002; Wang and Wang, 2003). A number of studies have shown that the properties of mammalian sodium channels are affected by pyrethroid concentrations in the 1 to 100 μM range (Motomura and Narahashi, 2001; Soderlund and Lee, 2001; Spencer et al., 2001; Wang et al., 2001; de la Cerda et al., 2002). Dose-response experiments with mammalian sodium channels have demonstrated K_d values that range from 0.44 to 95 μM for deltamethrin, a type II pyrethroid, and tetramethrin, a type I pyrethroid (Tatebayashi and Narahashi, 1994; Vais et al., 2000). The type I pyrethroid allethrin caused significant modifications of mammalian sodium channels at 10 μM (Ginsburg and Narahashi, 1999).

Sodium channels are closely related evolutionarily to voltage-gated calcium channels and have a similar predicted

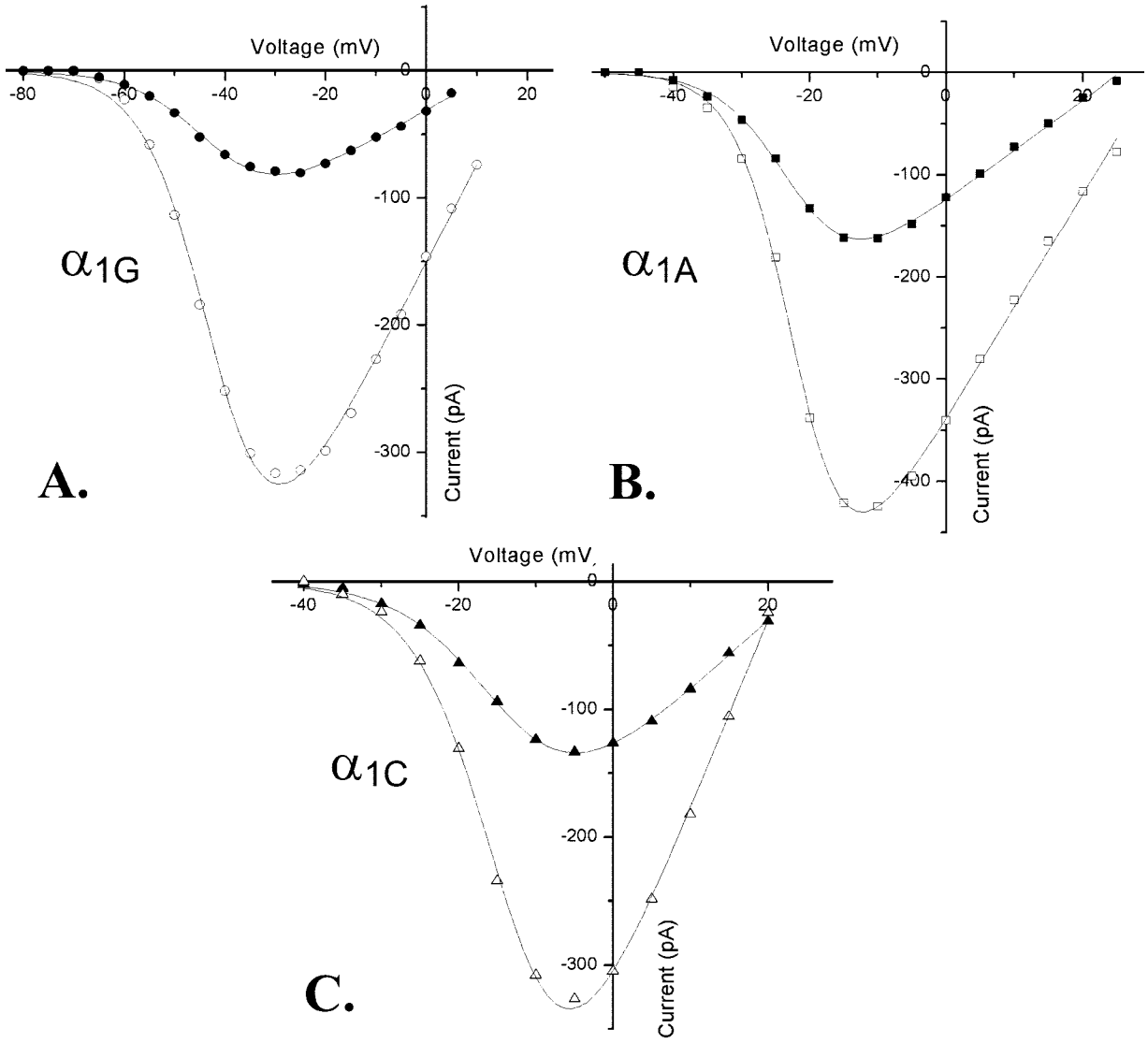

Fig. 6. Allethrin does not affect voltage-dependent activation of calcium channels. Current-voltage data were analyzed to determine the activation properties of the calcium currents. A, the voltage for half activation (V_{50act}) was not significantly different for control or allethrin-treated α_{1G} currents (control V_{50act} = −41.3 ± 0.7 mV, n = 12; 10 μM allethrin V_{50act} = −40.8 ± 0.5 mV, n = 12). B, allethrin does not significantly shift activation of α_{1A} currents (control V_{50act} = −19.3 ± 1.6 mV, n = 9; 20 μM allethrin V_{50act} = −20.1 ± 1.7 mV, n = 9). C, there was no significant change in the current-voltage relation of the α_{1C} currents exposed to allethrin (control V_{50act} = −13.9 ± 1.5 mV, n = 13; 10 μM allethrin V_{50act} = −13.6 ± 1.3 mV, n = 13). Note that in all three graphs shown above, allethrin-treated cells are shown with filled symbols whereas controls are shown with open symbols. The whole-cell current values for each point were divided by the maximal current to give normalized current on the y-axis of each graph.

structure (for review, see Catterall, 2000). The type I pyrethroid tetramethrin has been shown to block T-type calcium channels in rabbit sino-atrial node cells at 0.1 to 50 μM (Hagiwara et al., 1988; Satoh, 1995). In the present study, we report for the first time a comprehensive analysis of the effects of the type I pyrethroid allethrin on the three major classes of mammalian voltage-gated calcium channels expressed in HEK cells. The IC_{50} values for the three types of calcium channels studied were all approximately 7 μM. These concentrations are in the same range as the values for pyrethroid modification of sodium channels and suggest that calcium channels would be affected to an equal extent during pyrethroid poisoning.

In our study, we found that there were small but significant differences in the action of pyrethroids on the three classes of calcium channels examined. The three channel types represented the three main groupings of calcium channels based upon molecular similarity and physiological properties. The α_{1C} ($Ca_v1.2$) subtype represents the high-voltage activated, L-type dihydropyridine-sensitive channels; the α_{1A} ($Ca_v2.1$) subtype represents the high-voltage activated, P/Q-type ω-agatoxin IVA sensitive channels; and the α_{1G} ($Ca_v3.1$) subtype represents the low-voltage activated, T-type channels (Catterall, 2000). Allethrin caused a similar potent (IC_{50} $\sim$ 7 μM), reversible block of all three classes of calcium channels (Figs. 1 and 2). It has been shown previously that the effects of allethrin on sodium channels are reversible after washout (Ginsburg and Narahashi, 1999). Some interesting differences were noted, including a stimulation frequency-dependent increase in allethrin block for α_{1A} and α_{1C} currents, whereas no such effect was observed for α_{1G} (Fig. 3). Frequency-dependent effects of pyrethroids on voltage-gated sodium channels have been observed (Vais et al., 2001, 2003; Wang and Wang, 2003). The inherent differences in the inactivation properties (see below) of the low-voltage-activated α_{1G} channels compared with high-voltage- activated α_{1A} and α_{1C} channels may contribute to this difference (Catterall 2000; McRory et al., 2001).

Pyrethroids Have Differential Effects on Calcium Channels Compared with Sodium Channels. A number of studies have shown that pyrethroids cause delayed inactivation and slowed deactivation of sodium channels resulting in longer channel openings and leading to overstimulation of nerves and eventual paralysis (for review, see Zlotkin, 1999; Vais et al., 2001; Soderlund et al., 2002; Wang and Wang, 2003). Tetramethrin, a type I pyrethroid, causes these effects when applied to single sodium channels from rat hippocampal neurons (Motomura and Narahashi, 2001). Unlike that found for sodium channels, we find that calcium channel whole-cell currents are blocked by pyrethroids, which would result in less current and subsequently less calcium influx into neurons (or other cells affected). In addition to blockade, allethrin also caused distinct kinetic changes to the calcium channel whole-cell currents. Allethrin caused a distinct acceleration of calcium channel inactivation, which is the opposite of the pyrethroid effect on sodium channels (Martin et al., 2000; Vais et al., 2000). The acceleration of inactivation by allethrin is most pronounced in the more slowly inactivating α_{1A} and α_{1C} channels, compared with the normally fast inactivating α_{1G}. Both insect and mammalian sodium channels show a pronounced slowing of deactivation of the tail currents after a depolarizing pulse after exposure to pyrethroids (Martin et al., 2000; Zhao et al., 2000; Motomura and Narahashi, 2001; Soderlund and Lee, 2001; de la Cerda et al., 2002). In contrast, all three classes of calcium channels showed no significant changes in their tail current deactivation after exposure to allethrin.

Along with changes in the kinetics of inactivation, all three classes of calcium channels showed a pronounced hyperpolarized shift in their voltage-dependence of inactivation. Several studies have shown a small pyrethroid-induced hyperpolarizing shift in current-voltage relations and voltage-dependent inactivation of sodium currents (Smith et al., 1998; Spencer et al., 2001; de la Cerda et al., 2002). In contrast, the three classes of calcium channels examined showed no significant change in their current-voltage relations. Both the acceleration of inactivation and hyperpolarized shift in inactivation of calcium channels exposed to pyrethroids would be predicted to make fewer channels available for opening during subsequent depolarizing pulses and would cause a decrease in the overall calcium current.

Analysis of pyrethroid-resistant mutant insects have shown that parts of the S4-S6 transmembrane regions on insect sodium channels seem to be important binding sites for pyrethroids (Vais et al., 2000, 2001). These regions are important for the voltage-dependent, kinetic, and ion selectivity properties of both sodium and calcium channels (Catterall, 2000; Vais et al., 2001). Pyrethroids are thought to interact with the hydrophobic interior of the plasma membrane and bind to parts of the S4-S6 regions (Wang and Wang, 2003). Although the putative binding sites for pyrethroids are not conserved at the amino acid level between sodium and calcium channels, the overall structural similarity in these regions is conserved; thus, it would be of interest to identify the residues in calcium channels that are implicated in pyrethroid binding and functional modification.

Physiological Implications of Pyrethroid Exposure. The widespread use of pyrethroids has made it essential to determine the molecular targets of these chemicals to evaluate the risks of their use. A recent concern for exposure of the general population to pyrethroids is the spraying of suburban areas for mosquito control to lower the risk for West Nile virus transmission (Thier, 2001). Because pyrethroids have generally low acute mammalian toxicity, they have been one of the pesticides of choice for adult mosquito control (Thier, 2001). The agricultural use of pyrethroids may also expose humans to pyrethroids. Studies have found pyrethroid residues on vegetables (Kumari et al., 2002), and suburban residents with no occupational exposure to pyrethroids have been shown to have metabolites of these compounds in their urine (Schettgen et al., 2002). Our results suggest that at subacute doses, pyrethroids may affect both sodium and calcium channels. Since calcium channels are essential for maintaining calcium homeostasis in many cells, it is possible that these channels underlie some of the symptoms of chronic pyrethroid exposure. Rats chronically exposed to the type I pyrethroid permethrin for 45 days showed decreased sensorimotor performance and changes in acetylcholine receptor density in their brains (Abou-Donia et al., 2001). These effects could be consistent with blockade of different calcium channels types in specific areas of the brain. Blockade of T-type calcium channels could have profound inhibitory effects on electrical excitability in the brain and rhythmicity in the heart (Catterall, 2000; McRory et al.,

2001; Perez-Reyes, 2003). Pyrethroid effects on P/Q-type channels could suppress neurotransmission and affect long-term synaptic function by altering gene expression (Sutton et al., 1999; Catterall, 2000). In addition, the suppression of L-type channels by pyrethroids could affect excitation-contraction coupling, hormone secretion, and gene regulation (Catterall, 2000; Dolmetsch et al., 2001). In fact, several studies have already shown that pyrethroids can suppress gene expression (Ahlbom et al., 1994; Imamura et al., 2000, 2002). Imamura et al. (2000, 2002) showed that c-fos and brain-derived neurotrophic factor gene expression was suppressed in vitro and in vivo after exposure to the type I pyrethroid permethrin. Furthermore, they determined that the blockade of L-type calcium channels was responsible for this effect. Although it is clear from previous studies that many of the symptoms of pyrethroid toxicity are likely caused by their effect on voltage-gated sodium channels, our study suggests that blockade of voltage-gated calcium channels may also play a role.

Taken together, it seems prudent to suggest that a more detailed understanding of the actions of pyrethroids on ion channels and other potential molecular targets should be undertaken to ensure that the risk factors for chronic health problems from using these insecticides are better understood.

Acknowledgments

We thank Dr. Esperanza Garcia for help with cell culture and electrophysiology experiments and Diane Burton and the rest of the Department of Biology at the University-College of the Fraser Valley for assistance.

References

Abou-Donia MB, Goldstein LB, Jones KH, Abdel-Rahman AA, Damodaran TV, Dechkovskaia AM, Bullman SL, Amir BE, and Khan WA (2001) Locomotor and sensorimotor performance deficit in rats following exposure to pyridostigmine bromide, DEET, and permethrin, alone and in combination. *Toxicol Sci* **60:**305–314.

Ahlbom J, Fredriksson A, and Eriksson P (1994) Neonatal exposure to a type-I pyrethroid (bioallethrin) induces dose-response changes in brain muscarinic receptors and behaviour in neonatal and adult mice. *Brain Res* **645:**318–324.

Catterall WA (2000) Structure and regulation of voltage-gated Ca2+ channels. *Annu Rev Cell Dev Biol* **16:**521–555.

de la Cerda E, Navarro-Polanco RA, and Sanchez-Chapula JA (2002) Modulation of cardiac action potential and underlying ionic currents by the pyrethroid insecticide deltamethrin. *Arch Med Res* **33:**448–454.

Dolmetsch RE, Pajvani U, Fife K, Spotts JM, and Greenberg ME (2001) Signaling to the nucleus by an L-type calcium channel-calmodulin complex through the MAP kinase pathway. *Science (Wash DC)* **294:**333–339.

Forshaw PJ, Lister T, and Ray DE (2000) The role of voltage-gated chloride channels in type II pyrethroid insecticide poisoning. *Toxicol Appl Pharmacol* **163:**1–8.

Ginsburg K and Narahashi T (1999) Time course and temperature dependence of allethrin modulation of sodium channels in rat dorsal root ganglion cells. *Brain Res* **847:**38–49.

Hagiwara N, Irisawa H, and Kameyama M (1988) Contribution of two types of calcium currents to the pacemaker potentials of rabbit sino-atrial node cells. *J Physiol (Lond)* **395:**233–253.

Hamill OP, Marty A, Neher E, Sakmann B, and Sigworth FJ (1981) Improved patch-clamp techniques for high-resolution current recordings from cells and cell-free membrane patches. *Pflueg Arch* **391:**85–100.

Imamura L, Hasegawa H, Kurashina K, Hamanishi A, Tabuchi A, and Tsuda M (2000) Repression of activity-dependent c-fos and brain-derived neurotrophic factor mRNA expression by pyrethroid insecticides accompanying a decrease in Ca(2+) influx into neurons. *J Pharmacol Exp Ther* **295:**1175–1182.

Imamura L, Hasegawa H, Kurashina K, Matsuno T, and Tsuda M (2002) Neonatal exposure of newborn mice to pyrethroid (permethrin) represses activity-dependent c-fos mRNA expression in cerebellum. *Arch Toxicol* **76:**392–397.

Kakko I, Toimela T, and Tahti H (2003) The synaptosomal membrane bound ATPase as a target for the neurotoxic effects of pyrethroids, permethrin, and cypermethrin. *Chemosphere* **51:**475–480.

Kumari B, Madan VK, Kumar R, and Kathpal TS (2002) Monitoring of seasonal vegetables for pesticide residues. *Environ Monit Assess* **74:**263–270.

Martin RL, Pittendrigh B, Liu J, Reenan R, ffrench-Constant R, and Hanck DA (2000) Point mutations in domain III of a Drosophila neuronal Na channel confer resistance to allethrin. *Insect Biochem Mol Biol* **30:**1051–1059.

McRory JE, Santi CM, Hamming KS, Mezeyova J, Sutton KG, Baillie DL, Stea A, and Snutch TP (2001) Molecular and functional characterization of a family of rat brain T-type calcium channels. *J Biol Chem* **276:**3999–4011.

Motomura H and Narahashi T (2001) Interaction of tetramethrin and deltamethrin at the single sodium channel in rat hippocampal neurons. *Neurotoxicology* **22:**329–339.

Perez-Reyes E (2003) Molecular physiology of low-voltage-activated t-type calcium channels. *Physiol Rev* **83:**117–161.

Satoh H (1995) Role of T-type Ca2+ channel inhibitors in the pacemaker depolarization in rabbit sino-atrial nodal cells. *Gen Pharmacol* **26:**581–587.

Schettgen T, Heudorf U, Drexler H, and Angerer J (2002) Pyrethroid exposure of the general population-is this due to diet. *Toxicol Lett* **134:**141–145.

Smith TJ, Ingles PJ, and Soderlund DM (1998) Actions of the pyrethroid insecticides cismethrin and cypermethrin on house fly Vssc1 sodium channels expressed in Xenopus oocytes. *Arch Insect Biochem Physiol* **38:**126–136.

Soderlund DM, Clark JM, Sheets LP, Mullin LS, Piccirillo VJ, Sargent D, Stevens JT, and Weiner ML (2002) Mechanisms of pyrethroid neurotoxicity: implications for cumulative risk assessment. *Toxicology* **171:**3–59.

Soderlund DM and Lee SH (2001) Point mutations in homology domain II modify the sensitivity of rat Nav1.8 sodium channels to the pyrethroid insecticide cismethrin. *Neurotoxicology* **22:**755–765.

Spencer CI, Yuill KH, Borg JJ, Hancox JC, and Kozlowski RZ (2001) Actions of pyrethroid insecticides on sodium currents, action potentials and contractile rhythm in isolated mammalian ventricular myocytes and perfused hearts. *J Pharmacol Exp Ther* **298:**1067–1082.

Sutton KG, McRory JE, Guthrie H, Murphy TH, and Snutch TP (1999) P/Q-type calcium channels mediate the activity-dependent feedback of syntaxin-1A. *Nature (Lond)* **401:**800–804.

Tatebayashi H and Narahashi T (1994) Differential mechanism of action of the pyrethroid tetramethrin on tetrodotoxin-sensitive and tetrodotoxin-resistant sodium channels. *J Pharmacol Exp Ther* **270:**595–603.

Thier A (2001) Balancing the risks: vector control and pesticide use in response to emerging illness. *J Urban Health* **78:**372–381.

Vais H, Atkinson S, Eldursi N, Devonshire AL, Williamson MS, and Usherwood PN (2000) A single amino acid change makes a rat neuronal sodium channel highly sensitive to pyrethroid insecticides. *FEBS Lett* **470:**135–138.

Vais H, Atkinson S, Pluteanu F, Goodson SJ, Devonshire AL, Williamson MS, and Usherwood PN (2003) Mutations of the para sodium channel of Drosophila melanogaster identify putative binding sites for pyrethroids. *Mol Pharmacol* **64:**914–922.

Vais H, Williamson MS, Devonshire AL, and Usherwood PN (2001) The molecular interactions of pyrethroid insecticides with insect and mammalian sodium channels. *Pest Manag Sci* **57:**877–888.

Wang SY, Barile M, and Wang GK (2001) A phenylalanine residue at segment D3–S6 in Nav1.4 voltage-gated Na(+) channels is critical for pyrethroid action. *Mol Pharmacol* **60:**620–628.

Wang SY and Wang GK (2003) Voltage-gated sodium channels as primary targets of diverse lipid-soluble neurotoxins. *Cell Signal* **15:**151–159.

Zhao Y, Park Y, and Adams ME (2000) Functional and evolutionary consequences of pyrethroid resistance mutations in S6 transmembrane segments of a voltage-gated sodium channel. *Biochem Biophys Res Commun* **278:**516–521.

Zlotkin E (1999) The insect voltage-gated sodium channel as target of insecticides. *Annu Rev Entomol* **44:**429–455.

Address correspondence to: Dr. Anthony Stea, Department of Biology, University-College of the Fraser Valley, 33844 King Road, Abbotsford, British Columbia, Canada, V2S 7M8. E-mail: steat@ucfv.bc.ca